NRIAG JOURNAL OF ASTRONOMY AND GEOPHYSICS
2020, VOL. 9, NO. 1, 459–470
https://doi.org/10.1080/20909977.2020.1768324

Integrated prediction of deep-water gas channels using seismic coloured inversion and spectral decomposition attribute, West offshore, Nile Delta, Egypt

Amir Ismail [a,b], Hatem Farouk Ewida[c], Mohammad Galal Al-Ibiary[a] and Aldo Zollo [b]

[a]Department of Geology, Faculty of Science, Helwan University, Cairo, Egypt; [b]Department of Physics "E. Pancini", University of Naples 'Federico II', Italy; [c]Exploration General Manager, PERENCO North Sinai Petroleum Company, Cairo, Egypt

ABSTRACT

In the West Delta Deep Marine (WDDM) concession many important gas reservoirs have been recently discovered. To improve the possibility of discovering new natural gas resources, an integrated prediction method approach is used in this study to identify the deep-water gas reservoirs. Post-stack seismic coloured inversion and the spectral decomposition attribute, combined with composite logs of five wells, are used to indicate the lateral and vertical variations of the gas channels in El Wastani Formation. Data conditioning and petrophysical analysis are performed. Both techniques help and improve visual evidence to detect gas channels. Coloured inverted seismic profile show relatively low impedance zones represent the gas channels. Spectral decomposition attribute solves the problem related to thin gas-sand layers through three different frequency magnitude values. The spatial distribution of the gas-channels properties indicates a good calibration at the well location with the effective porosity in the range of 15–35%. Comparing the results of the coloured seismic inversion with the spectral decomposition attribute, the low-frequency range through the spectral decomposition analysis is consistent with the low impedance values represents the gas channels. Furthermore, the methodology followed in the current study is advantageous to identify the gas reservoirs in various basins with similar geological settings.

ARTICLE HISTORY
Received 29 November 2019
Revised 25 April 2020
Accepted 8 May 2020

KEYWORDS
Seismic inversion; offshore Nile Delta; gas channels; gas-bearing sand zones; spectral decomposition attribute; well logging

1. Introduction

Pettingill and Weimer (2002) clarified the importance of the exploration in the deepwater for a new hydrocarbon. The West Delta Deep Marine (WDDM) concession is located in the East Mediterranean Sea at around 50–100 km west offshore, Egypt, and covers 6150 km2 of the Northwest margin of the Nile cone. The production in this area represents around two-thirds of the gas production in Egypt. In the Nile Delta province, approximately 88 Trillion Cubic Feet (TCF) of gas reserves have already been discovered includes new significant discoveries such as the Zohr field. Geological information of the Nile delta is still insufficient and need more exploration activities in the future because of the limited subsurface data. Gas is originated and trapped at stratigraphic traps extending from the Lower Miocene to the Lower Pliocene. Multitrillion cubic feet of new gas discoveries in the east, centre, and west offshore Nile Delta Basin over the last few years (Barsoum et al. 2002; Niazi and Dahi 2004). Reilly (2016) pointed out the difficulty of the identification of deep-water reservoirs which represents a challenge where the depositional system with more complexity and limited exploration level. Seismic inversion and different classes of seismic attributes analysis are two significant techniques to depict reservoir characteristics (Pendrel, 2006a; Chopra and Marfurt 2007). The WDDM concession (Figure 1) was obtained in 1995 by both BG Group and Edison Gas.

Stratigraphic hydrocarbon reservoirs are often in the form of sand deposits associated with channels. Therefore, the identification of channels by using modern techniques important to improve seismic data imaging and interpretation. Khalid et al. (2014) pointed out the importance of separating the gas-saturated sand intervals from different lithologies from the interpretation of seismic data. Khalid and Ghazi (2013) described the complexity to distinguish and discriminate between the payable hydrocarbon interval from non-payable intervals by using the traditional seismic data interpretation. For this reason, different techniques are used together to give the best results. At the scarab field there are two main channels, were classified based on their age where channel 2 is older than channel 1. Both channels have the same depositional environments but with different trending directions (Figure 1).

Ozdemir (2008) explained the importance of the coloured seismic inversion as a fast and accurate technique to convert the original reflectivity of different

CONTACT Amir Ismail amir_ismail@science.helwan.edu.eg Department of Geology, Faculty of Science, Helwan University, Cairo, Egypt

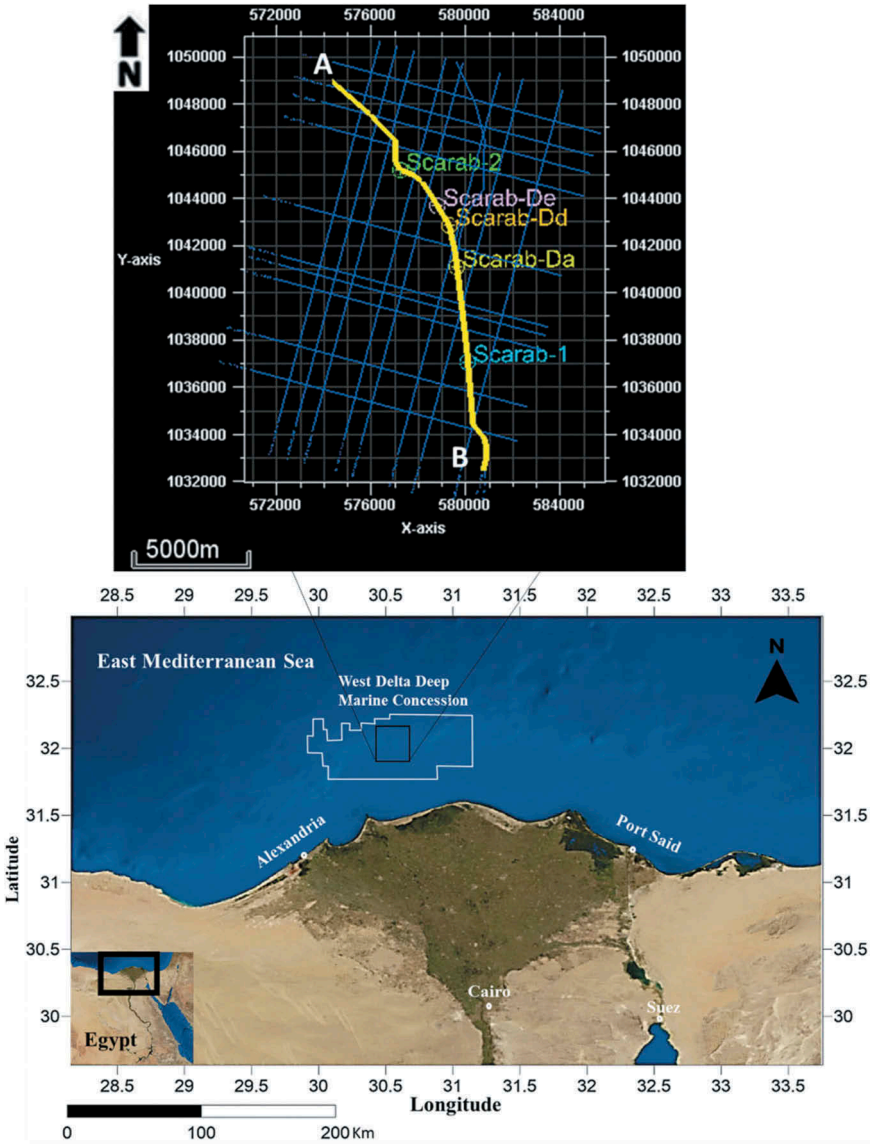

Figure 1. Map of Egypt show the location of West Delta Deep Marine (WDDM) concession with locations of five wells and the 2D-seismic arbitrary line (AB) used in the study with yellow colour, modified after Ismail et al. 2020b.

seismic features, horizons, and geological structures data into a rock and layer property based on its impedance. Different rock's elastic properties can be computed through the petrophysical properties by using saturation, porosity, and lithology logs such as gamma ray log through the analysis. Seismic coloured inversion proceeds obviously better and faster than traditional seismic inversion methods like model-based inversion and band-limited inversion methods (Lancaster and Whitcombe 2000b). Moreover, other seismic inversion methods are more expensive and not proceeded routinely by the user. Traditional seismic inversion methods are expensive, require specialists, and performed routinely without pursuit from the interpreter, whereas Seismic Coloured Inversion (SCI) is rapid and robust (Chung and Lawton 1995). The post-stack seismic acoustic impedance inversion is widely used to predict quantitatively and identify qualitatively reservoirs characterisations (Gholami 2016). The coloured inversion with great importance in the hydrocarbon exploration strategy as it is working without needing a background model and it can discriminate between the layer boundaries of soft and hard rock formations along fluid fill pattern of the subsurface geology (Datta Gupta and Gupta 2017).

In the SCI method, the input seismic data with zero phase, and use an operator (O) in the time domain to transform seismic traces (S) into impedance (I); (I = O* S). This operator can be used with the seismic data through the convolution algorithm to define the amplitude spectrum into the impedance spectrum of subsurface different layers. This operator has a – 90° phase (Neep 2007). Hence, the operator integrates the reflectivity series into impedance. Pendrel, (2006b) analysed carefully various seismic and well log spectra to detect the coloured inversion operator that used to transform the seismic trace to an average impedance log.

The inverted seismic data is strongly based on both user-defined bandwidth of the seismic data and the precision computation and extraction of the initial low-frequency impedance model (Ghosh 2000; Ten Kroode et al. 2013). To retrieve and enhance the values of the absolute impedance, the low frequencies values that lost from the seismic data are often regained after the interpolation of low-pass-filtered impedance well log data supported by the information from both interpreted horizons and different seismic features (Hansen et al. 2008; Karimi et al. 2017).

Castagna et al. (2003) applied a similarity track decomposition technique for instantaneous spectral analysis to identify and track low-frequency shadows at the bottom interface of hydrocarbon reservoirs. The Spectral Decomposition (SD) approach is of great importance in the thin hydrocarbon reservoirs identification from the seismic data (Goloshubin et al. 2014). Rastogi (2013) extracted discrete-frequency energy cubes by using windowed spectral analysis which can be used to identify and interpret the reservoir's characteristics. Hardy et al. (2003) demonstrated that the average frequency characteristics delivered from seismic data are fitting firmly with shale volume in a specific region. The 2D seismic profile can produce helpful SD analysis using short windows for transforming and displaying the frequency spectra.

Identification of the hydrocarbon-bearing reservoirs in the Nile Delta Basin represents a challenge with high expected risk (Mohamed et al. 2015; El Khadragy et al. 2017; Ismail et al. 2020a; Ismail et al. 2020b). Therefore, in this paper, we present an integration between the full stack SCI and SD attribute combined with the wireline logs of Scarab-Dd, Scarab-Da, Scarab-De, Scarab-2, and Scarab-1 wells are used to reduce the exploration risk of the identification of deep-water gas channels.

2. Geology of the area

The thickness of the Early Miocene in the west to east of the central part, offshore, Nile delta is affected by the extension of block faulting and the erosion of the upper interface during the Late-Middle Miocene uplift (EGPC 1994). Source rocks are formed in the Late Mesozoic to Early Miocene sediments (Vandré et al. 2007) and in the Upper Cretaceous black shales that saturated with high Total Organic Content (TOC) represent high-quality source rocks (Abdel Aal et al. 2000).

Abdel Aal et al. (2000) described the major structural setting of the WDDM area shows that it is a fault-bounded block with the complex interplay among three main fault trends; the southwest-northeast trending Rosetta fault which is the largest in the WDDM region and it is orientated extensional to strike-slip. Wells used in this study (Figure 1) reaches the Upper Miocene, and for this reason, the available data that demostrate the geologic history for pre-Lower Miocene based on the recent studies which provide more information interpreted from the gravity and seismic surveys about Nile Delta.

Moreover, the structural behaviour has been studied by many authors (e.g. Saleh 2013; Hanafy et al. 2017). Emphasis on clear investigating the offshore Nile Delta Basin, based on structure, hydrocarbon potential, and stratigraphy (e.g. Wescott and Boucher 2000; Marten et al. 2004). The Neogene-Quaternary sediments (Figure 2) are classified into three depositional cycles; a Miocene cycle is represented by Sidi Salim, Qawasim, and Rosetta formations; a Pliocene-Pleistocene other cycle is represented by Abu Madi, Kafr El Sheikh, El Wastani, sand beds intercalated with shale (Rizzini et al. 1978), and Mit Ghamr formations; and an uppermost Holocene cycle is represented by Bilqas Formation (Schlumberger 1984; Abu El-Ella 1990).

3. Methodology

Identification of thin gas zones and channels using 2D post-stack seismic data analysis is very challenging in West Delta Deep Marine (WDDM). The thickness of sandstone reservoir intervals at different zones along the area is close to the resolution limit of the seismic data. In this study, the analysis was supported by different logs of five wells (Scarab-Dd, Scarab-Da, Scarab-De, Scarab-2, and Scarab-1). The petrophysical analysis is performed for two wells (Scarab-Da and Scarab-De) and proved as productive wells with a suite of wireline logs such as Vp sonic log, resistivity, and gamma-ray. Seismic data conditioning, Wavelet extraction, and synthetic seismograms were extracted to have an accurate tie and pick Bilqas/Mit Ghamr Formation, El Wastani Formation, channels 1 and 2 and geological structures before starting the coloured seismic inversion and spectral decomposition analysis. The overall analysis scheme for coloured seismic inversion analysis is summarised in (Figure 3).

3.1. Seismic to well tie

In the first step, check-shot correction and the extraction of a statistical wavelet has been done to create synthetic seismograms using the 2D post-stack seismic data supported by all five wells. This is used to detect the corrected depth to TWT of all formation tops on seismic data. The wavelet provides an optimum seismic to well log tie has a characteristic phase, frequency, and amplitude which represent the main parameters through the seismic interpretation using advanced techniques like seismic attributes and seismic inversion analysis. The seismic wavelet is commonly obtained using statistical method (Nanda 2016). This process requires comparing the real

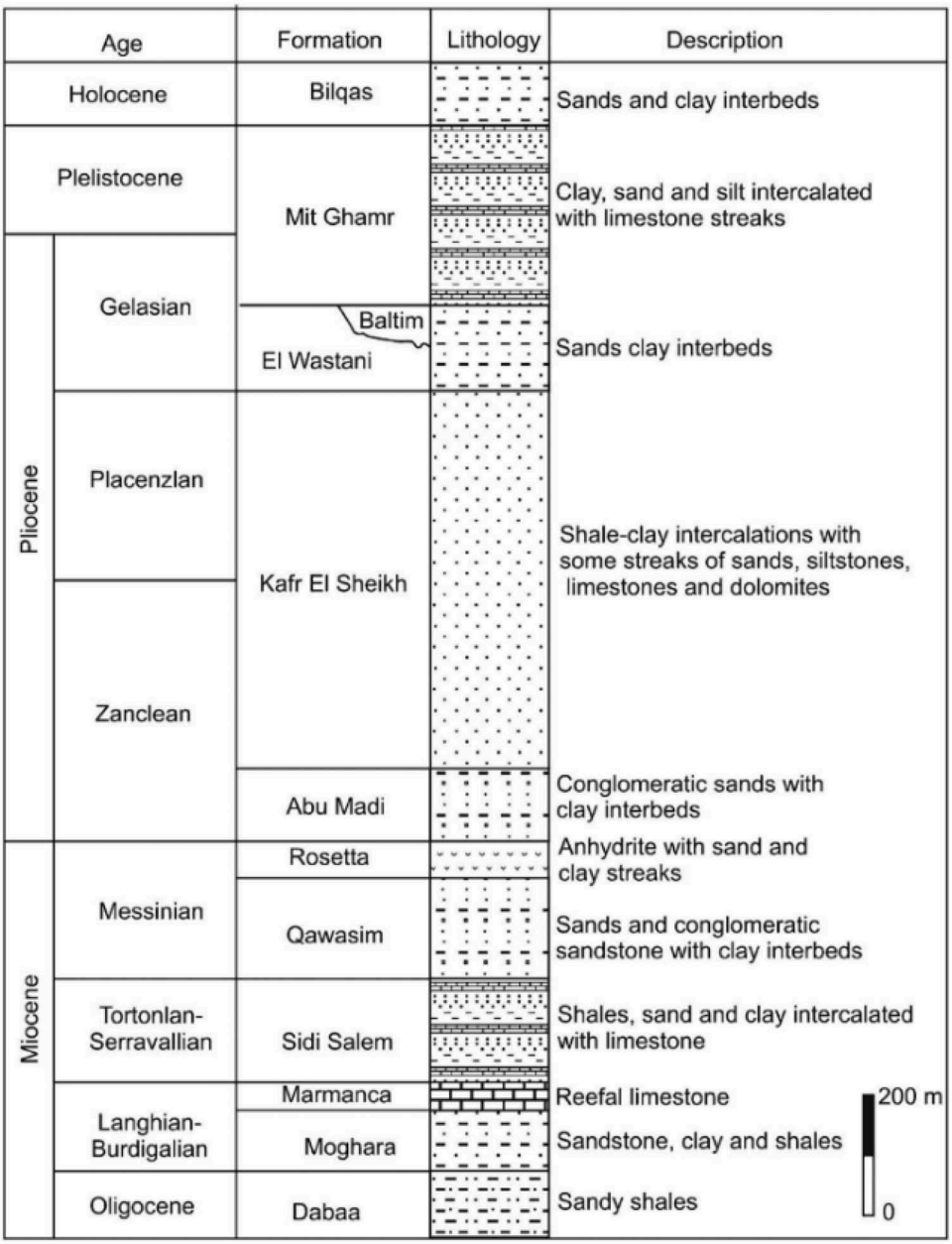

Figure 2. Nile delta stratigraphic column (Younis et al. 2015).

seismic data and well-logs responses with the synthetic trace (Figure 4). Chopra and Sharma (2016) shows that if the calibration results provide a good matching through the correlation with fresnel zone parameter consideration, then the seismic can be in terms of geology. If the calibration results were not accurate, Therefore, the interpretation of seismic data still with major uncertainty. The process of statistical wavelet extraction uses auto-correlation, and implies a constant phase defined by the user. A zero-phase is assumed as the seismic processing would have performed that by convolving the seismic data to an inverse filter that converts the estimated wavelet in the data into an equivalent of zero-phase. The extracted wavelet phase has a reversed SEG polarity (Figure 4). The extraction of a statistical wavelet is performed in the time window where the seismic and synthetic reflectivity match reliably. A constant 600 ms computation window (between 1700 ms to 2300 ms), 200 ms in length with a taper of 25 ms. Subsequently, a synthetic seismogram is created using the same parameters (Figure 4).

3.2. Petrophysical analysis

Prediction of Gas channels is carried out by analysing the composite logs of two wells (Scarab- Da and Scarab-De) (Figures 5 and 6). Shale volume (V_{sh}) helps to discriminate between the reservoir and non-reservoir rock (Schlumberger 1984). V_{sh} is calculated from gamma ray log by the formula (Equation 1) below (Asquith and Gibson 1982):

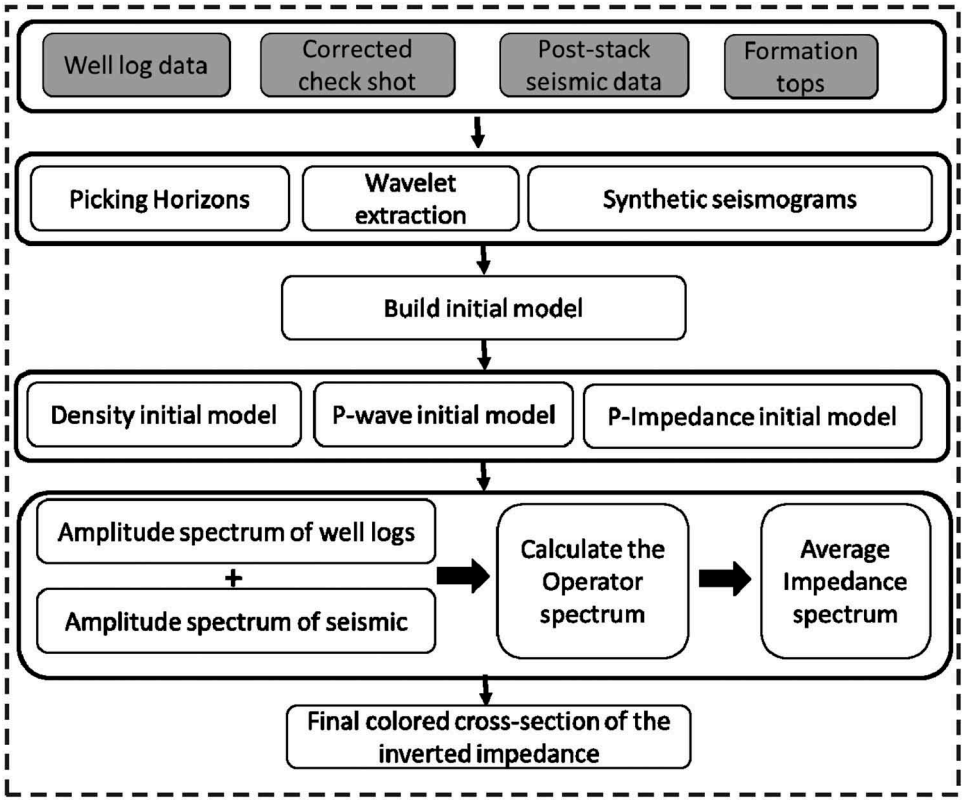

Figure 3. Flow chart outlining the steps of the coloured seismic post-stack inversion workflow performed in this study.

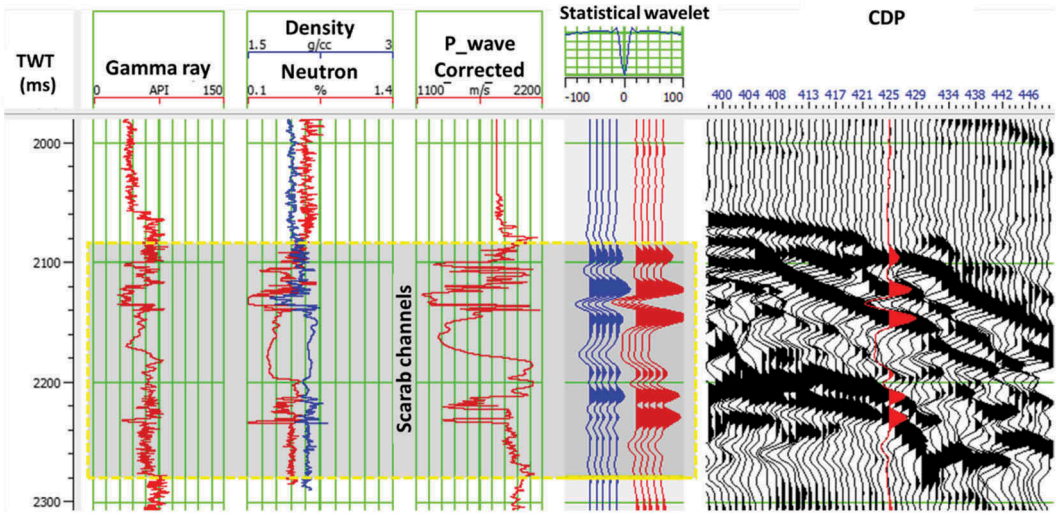

Figure 4. An example of the well-tie of Scarab-De well. The blue seismic traces are the calculated synthetic and the red represents the real seismic data using statistical wavelet with time response on top and the phase is constant 180 degrees for post-stack seismic data.

$$IG_{GR} = \frac{GR_{log} - GR_{min}}{GR\,\max - GR_{min}} \qquad \text{(Equation1)}$$

where I_{GR} = gamma ray index, that can be related and corrected to shaliness.

GR_{log} = gamma ray reading of formation; GR_{min} = minimum gamma ray; GR_{max} = maximum gamma ray.

Neutron-density (porosity) logs are used to calculate the total porosity (Schlumberger 1984), whereas the effective porosity (PHIE) is calculated and corrected for shale volume. Water saturation S_w is calculated to estimate the hydrocarbon saturation of the targeted intervals. Indonesian equation is used to calculate the water saturation by Equation (2) (Worthington 1985):

$$Sw^{n/2} = \frac{\sqrt{1/Rt}}{\frac{Vcl^{\left(1-\frac{Vcl}{2}\right)}}{\sqrt{Rcl}} + \frac{\sqrt{\emptyset_e^m}}{\sqrt{a*Rw}}} \qquad \text{(Equation2)}$$

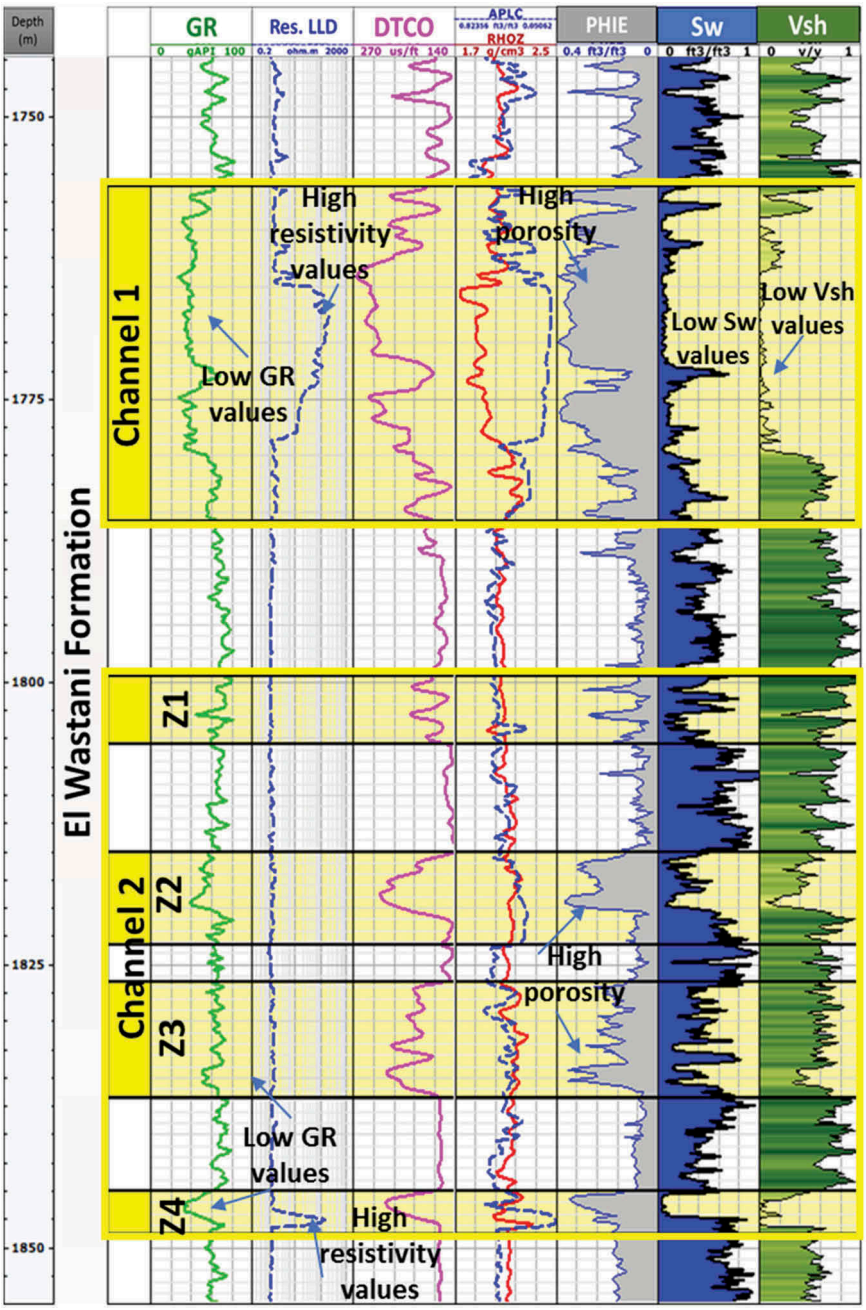

Figure 5. Porosity (PHIE), water saturation (Sw), and volume of shale (Vsh) calculations for Scarab-De well identify Channels 1 and gas zones z1, z2, z3, and z4 in channel 2 with yellow colour. The gas zones are characterised by low values of water saturation and volume of shale and with medium to high resistivity (LLD), and high porosity (PHIE) values.

where Sw = water saturation; Rt = true formation resistivity; Vcl = shale volume; Rcl = shale resistivity; ϕe = effective porosity; Rw = formation water resistivity; m = cementation exponent; a = tortuosity factor.

3.3. Seismic interpretation

Six horizons are structurally and stratigraphically interpreted after well to seismic tie and checkshots correction, including seabed surface (Bilqas/Mit Ghamr Formation), El Wastani Formation, top and base of Channel 1, and top and base of Channel 2. All horizons are smoothed and checked previously, the layers between horizons are built to be consistent with the depositional sequence (Figures 7).

3.4. Coloured inversion

The seismic coloured inversion can transform the seismic data into several coloured layers based on its rock physical properties. These properties are represented by the density, velocity, and acoustic impedance. Various methods of seismic inversion have been defined each with its advantages and disadvantages. Input data required for an inversion include time/depth-migrated pre/post-stack data, a convenient wavelet, initial earth models, and picked horizons in TWT (Veeken and Da

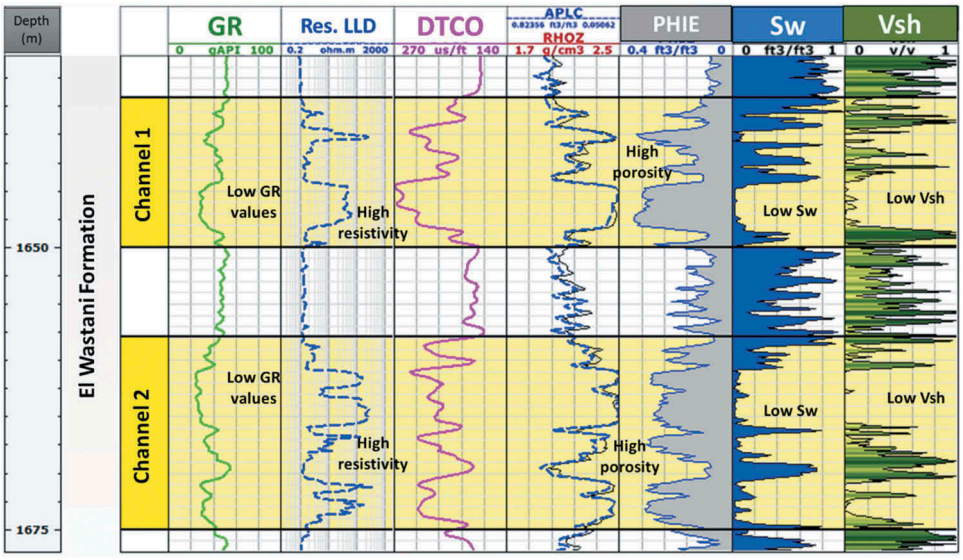

Figure 6. Porosity (PHIE), water saturation (Sw), and volume of shale (Vsh) calculations for Scarab-Da well identify Channels 1 and 2 with yellow colour. The gas zones are characterised by low values of water saturation and volume of shale and with high resistivity (LLD), and high porosity (PHIE) values.

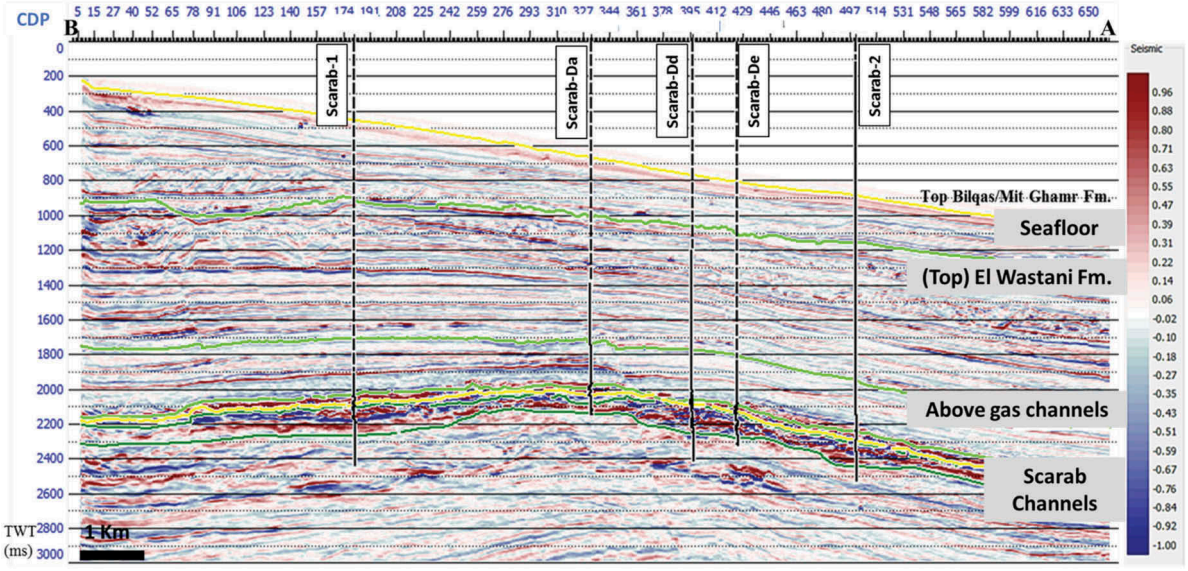

Figure 7. The original seismic line with six of horizons obtained from structural and stratigraphic interpretation after wells to seismic tie. The location of this traverse is shown in figure 1.

Silva 2004). The approach of using several seismic inversions is either deterministic or probabilistic in nature. The coloured inversion represents one of the best deterministic methods based on a special filtering technique. This technique provides higher detectability in impedance with respect to normal post-stack seismic data (Dai et al. 2004). In the inversion window, the amplitude spectrum of the log is compared with that of the seismic dataset. Thereafter, the operator is designed bringing the seismic amplitudes corresponding to those in the wells. This operator is posteriorly applied to the whole seismic data (Lancaster and Whitcombe 2000a). The operator is derived by computing the acoustic impedance and plot it against frequency for all wells in the area (Figure 8a). Furthermore, extract a fit regression line to the amplitude spectrum of the AI to represent the real subsurface impedance spectrum (Figure 8b). Computing the seismic spectrum from the nearest seismic traces to all wells. Consequently, both spectra used to derive the operator spectrum which transforms the seismic spectrum into the average impedance spectrum. Finally, the final spectrum is combined with a − 90° phase shift to create the required operator in the time domain (Figure 6c). The calculated operator in the frequency domain is represented in Figure 6(d).

A linear fit is performed as a shaping filter to calculate an exponential function (fα) (Velzeboer 1981). Thereafter, the filter can transform the seismic data into an assumed acoustic impedance equivalent. The hypothesis is made that the input seismic data with zero-phase.

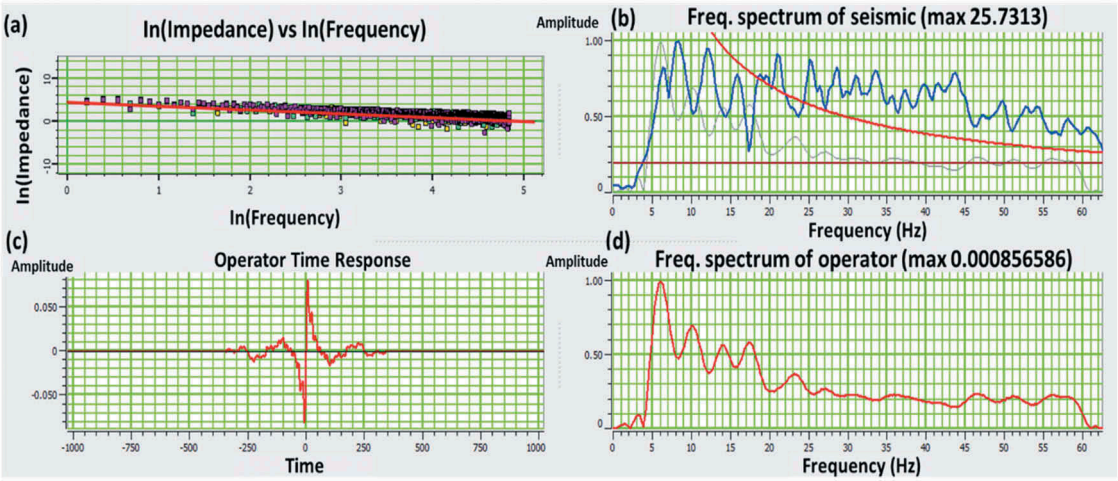

Figure 8. (a) Acoustic impedance from all five wells. (b) Seismic spectra near the wells (blue). The red-line corresponds to the fθ AI spectrum derived in (a). The operator spectrum (brown) is the ratio of these two spectra. (c) Time response of the operator and (d) Frequency spectrum of the operator from 5 to 60 HZ.

Quality of the correlation of the inverted results between the P-impedance, synthetic and seismic data using the inversion algorithm for all wells is illustrated in Figure 9 which shows good correlation values at all wells locations with an average value of correlation equal (0.9875). The parameters used in coloured inversion are as follows: Threshold for inverse = 2, operator length = 200, and taper length = 50.

3.5. Spectral decomposition

Frequency analysis is an advanced and promising discipline in geophysics and hydrocarbon exploration using seismic data set frequency behaviour. Furthermore, the frequency responses and their measurements are not similar, so it is important to integrate other data such as well-logs and extract suitable seismic attributes. Prior to extracting the spectral decomposition attribute, the Amplitude Spectrum is extracted for the full seismic data in Figure 10, where the seismic data peak frequency is about 30 Hz, and the frequency band is from 10 Hz to 90 Hz (Figure 8).

Frequency decomposition splits seismic trace energy into spectral sub-bands. Thus, each input seismic trace produces one output trace for each spectral sub-band, and the input 2D seismic section produces a separate 2D seismic section for each sub-band. In other words, spectral decomposition is the conversion

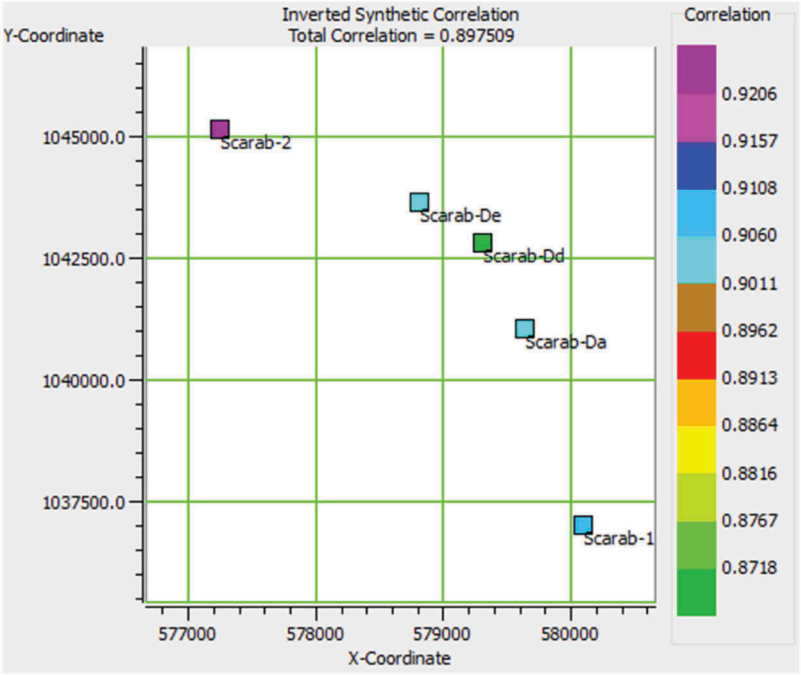

Figure 9. Correlation of the inverted results between the P-impedance, synthetic and seismic data using inversion algorithm for all wells.

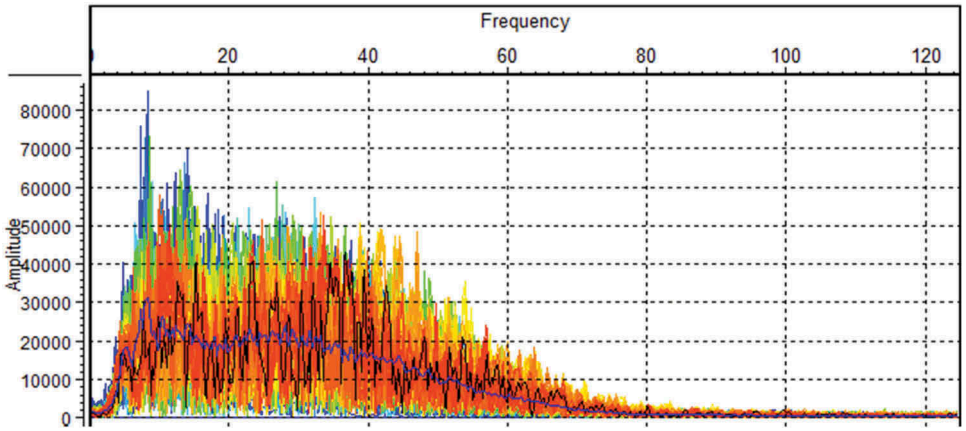

Figure 10. Amplitude spectrum and frequency analysis for the seismic traces. The blue line represents the graph average trace.

of seismic data into discrete frequencies/wavenumbers or frequency/wavenumber bands. Spectral decomposition (SD) is mostly used for layer thickness determinations and identifying stratigraphic variations. It has also helped identify the gas zones. Spectral decomposition using different mathematical methods such as Discrete Fourier transform (DFT) and Continuous Wavelet Transform (CWT) can convert the seismic data from the time into the frequency domain.

4. Results and discussion

Well-log interpretation is performed to evaluate the geological formation based upon its log response changes. Then, the correlation between nearby five wells data provides detailed information helpful for understanding the sub-surface geology. Detection of the gas intervals by various well-log analysis uses Resistivity (LLD), Gamma Ray (GR), and Vp sonic logs of two wells are achieved. Figures 5 and 6 shows that El Wastani Formation contains thin intervals of clean sands with minor shale content. Generally, the petrophysical analysis of Scarab-De well (Figure 5) shows that channel 1 is characterised by high resistivity and porosity as well as low water saturation and volume of shale values with a clear cross over in the neutron-density logs with good separation which may be due to the high gas content while channel 2 is characterised by lower resistivity and porosity values in comparison to channel 1. Moreover, the petrophysical analysis of Scarab-Da well (Figure 6) shows that both channels 1 and 2 are characterised by high resistivity and porosity as well as low water saturation and volume of shale values due to the high gas content. The selected zones with yellow colour, illustrate increasing in the resistivity (LLD) values and decreases in both Gamma-ray and P-wave velocity values as a typical signature and good sand saturated gas indicator. Gamma ray log records about 25–60 api on average through the gas bearing-sand zones. These sands have Rt in the range of 50–295 Ω-m and effective porosity in the range of 15–35%. Water saturation, porosity, and volume of shale values were calculated through the Petrophysical analysis and gave good evidence for hydrocarbon production.

Integrated analyses are of great importance to hydrocarbon development projects (Cosentino 2001), as well as post-stack SCI is one of the most important modern techniques for extracting more significant information from the seismic data. Inversion substitutes the seismic signature by a blocky response display based on elastic impedance layering which supports and assists the interpretation to give a more significant meaning of the geological and petrophysical boundaries in the subsurface. Veeken and Da Silva (2004), illustrated how seismic inversion can enhance the resolution of the seismic data in several cases and provide more information about the reservoir parameters.

4.1. Coloured inversion

The coloured inversion is performed using five wells available in the study area. We have derived the Operator (O) using 2D post-stack seismic data and well-log data as described in the methodology. Once the operator is designed, it is convolved with seismic trace to obtain the acoustic impedance. Since the well-data extends up to TWT equal to 2800 ms from the surface. The inversion of the seismic section shows impedance variation with time calculated using impedance model and log data from the sea-bed at 400 ms up to 2800 ms. At the well locations, the inverted impedance columns produced from seismic inversions are used to create synthetic traces (Maurya and Singh, 2015). Figure 11 illustrates the coloured inverted seismic section with relatively low impedance zones represents the gas channels in El Wastani formation with clearly observable showing colour variation from red to yellow colour in El Wastani formation at TWT from 1800 ms up to 2600 ms. Another relatively high impedance zone that is clearly visible in magenta colour can be related to the presence of water or abrupt change in the sand to shale volume in El Wastani formation, whereas the channel 2 is divided into four sub-channel zones as shown in Figure 5.

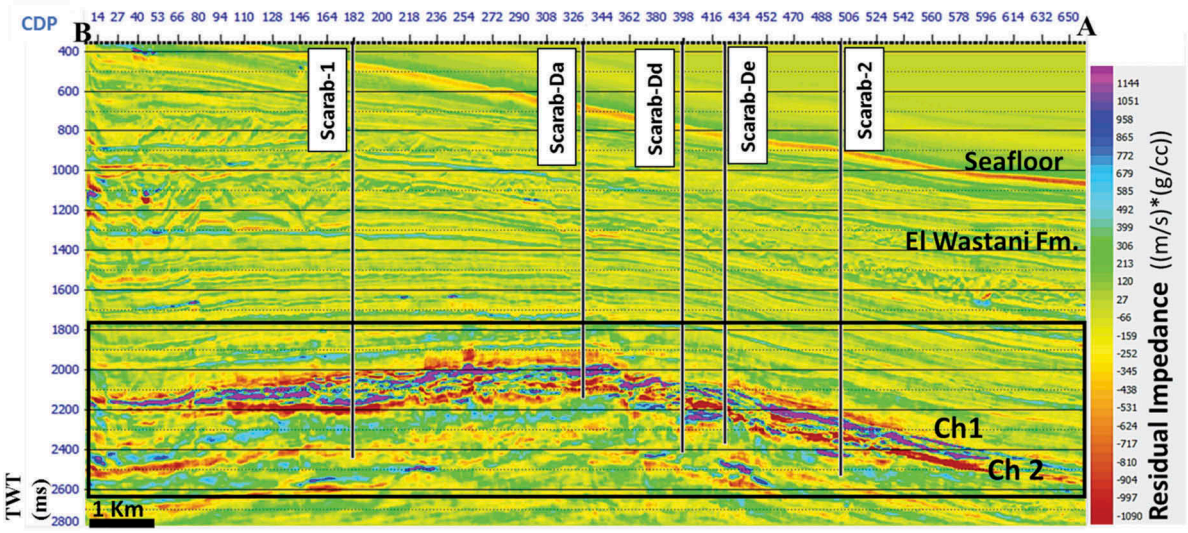

Figure 11. The estimated acoustic impedance seismic section using colored inversion. Gas channels are highlighted by the rectangle.

4.2. Spectral decomposition attribute

Seismic data have been changed from the time domain to the frequency domain using the DFT algorithm, and in turn, produced an amplitude tuning profile. The results show that the gas channels hardly represented within the low-frequencies range and high amplitudes. The three frequency ranges (Figure 12a, b, and c) are 10 Hz in Red colour, 35 Hz which represent the predominant frequency in Green colour, and 65 Hz in Blue colour.

The vertical section shows the RGB plot of seismic line A-B (Figure 12e) where the white arrows indicate the hydrocarbon reservoir. The results illustrate the frequencies differences with good contrasts are enhanced compared to the original seismic section and it worked as a good gas/hydrocarbon indicator where it provides clearly the gas channels along the seismic section (Figure 12e).

SD attribute is very helpful for solving the problem related to thin gas-sand layers. thus, thinner beds displayed better with higher frequency components while thicker beds with lower frequency through three different frequency magnitude values with red, green, and blue colours respectively were schemed and blended together with the result in Figure (11e) highlighting the variation in amplitude and frequency as variation in intensity and colour (McArdle and Ackers 2012).

5. Conclusion

In this study, we have presented the application of SD attributes and post-stack SCI to predict the deep-water

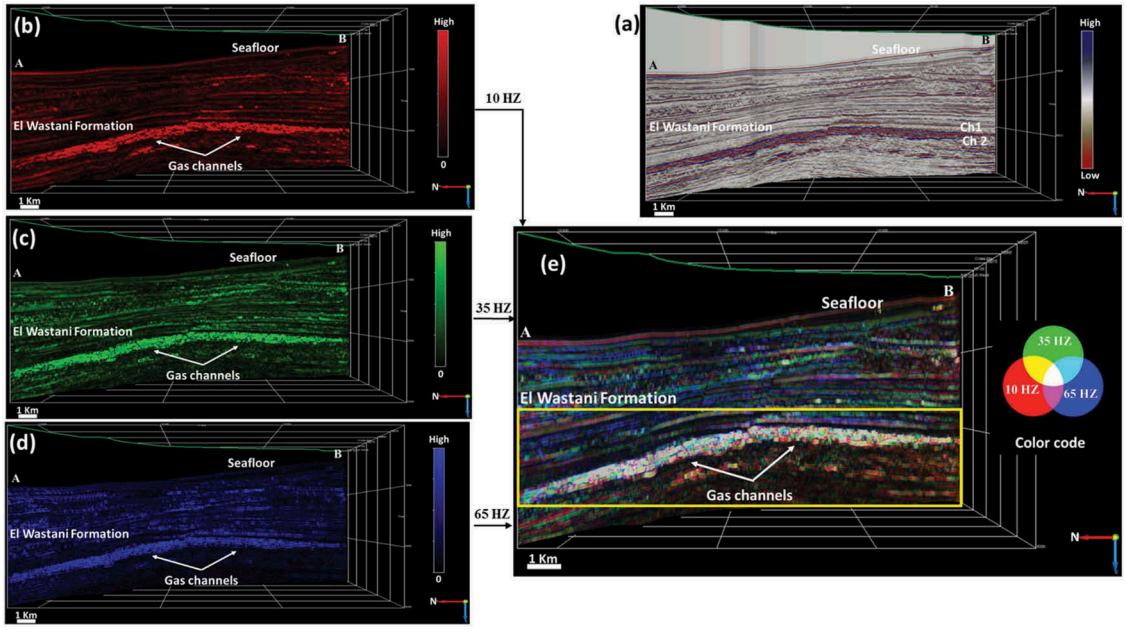

Figure 12. (a) Original seismic profile. (b, c, and d) with Red, Green and Blue values calculated by average output frequencies where the three frequency ranges are: 65 Hz in Blue color, 35 Hz in Green color, and 10 Hz in Red color respectively. (e) Final output with the three-color codes.

gas channels, West offshore, Nile Delta, Egypt. The main contribution of this work is providing a more detailed seismic reflection image through the integration of the spectral decomposition and the colour seismic inversion methods. According to the main aim of our work to identify the gas zones and channels in the target TWT zones of El Wastani Formation to separate gas from non-gas intervals and identify the gas channels. The results from the coloured inversion using 2D post-stack seismic data analyses provide a mutually consistent impedance section. The analysis estimated the low-impedance zone within gas channels zones in (Figure 11) which confirm the presence of sand channels and demonstrate the spatial distribution of the low impedances along the sand channel between 1800 ms and 2600 ms and provide a high-resolution image of the subsurface compare to the original seismic data.

Coloured seismic inversion analysis shows a good calibration with the well-logs and provides a clear contrast between the gas-bearing sand and the seal rocks based on the acoustic impedance values. Comparing the results of the coloured seismic inversion (Figure 11) with the spectral decomposition attribute (Figure 12), the low-frequency range through the SD results show a good matching with the low impedance values corresponding to the gas channels and gas zones.

The quantitative interpretation approach is one of the required interpretation processes for this kind of challenging geological set up towards finding gas-bearing sand. Coloured inversion is fast, cost-effective, and a quantitative interpretation technique and does not require any prior model.

Acknowledgements

This work is supported by a part of the Egyptian General Petroleum Corporation (EGPC) project in west offshore Nile Delta, Egypt. The authors are greatly thankful to Rashid Petroleum Company (RASHPETCO), the Egyptian General Petroleum Corporation (EGPC) for providing the data and for permission to publish this study, and to the Egyptian cultural affairs and missions sector to give the opportunity to the corresponding author to spent enough time at Seismological Laboratory (RISSC-Lab), Department of Physics E.Pancini, University of Naples "Federico II", Napoli, Italy.

Disclosure statement

The authors declare that the research was conducted in the absence of any commercial or financial relationships that could be construed as a potential conflict of interest.

ORCID

Amir Ismail http://orcid.org/0000-0003-1167-0483
Aldo Zollo http://orcid.org/0000-0002-8191-9566

References

Aal AA, El Barkooky A, Gerrits M, Meyer H, Schwander M, Zaki H. 2000. Tectonic evolution of the eastern mediterranean basin and its significance for hydrocarbon prospectivity in the ultradeepwater of the nile delta. The Leading Edge. 19(10):1086-1102. doi:10.1190/1.1438485.

Abu El-Ella R. 1990. The neogene-quaternary section in the Nile delta, Egypt: geology and hydrocarbon potential. J Pet Geol. 13(3):329–340. doi:10.1111/j.1747-5457.1990.tb00850.x.

Asquith G, Gibson C. 1982. Basic well log analysis for geologists. Tulsa (Oklahoma): he American Association of Petroleum Geologists.

Barsoum K, Della M, Kamal M. 2002. Gas chimneys in the Nile Delta slope and gas field occurrence. In: MOC 2002; Alex., Cairo.

Castagna JP, Sun S, Siegfried RW. 2003. Instantaneous spectral analysis: detection of low-frequency shadows associated with hydrocarbons. Lead Edge. 22 (2):120–127. doi:10.1190/1.1559038.

Chopra S, Marfurt KJ. 2007. Seismic attributes for prospect identification and reservoir characterization. Tulsa (Oklahoma): Society of Exploration Geophysicists.

Chopra S, Sharma RK. 2016. Preconditioning of seismic data prior to impedance inversion. Aapg Explorer. 37 (1):30-33.

Chung H, Lawton D. 1995. Frequency characteristics of seismic reflections from thin beds. Recorder. 31:32–37.

Cosentino L. 2001. Integrated reservoir studies. Paris: Technip; p. 310.

Dai J, Xu H, Snyder F, Dutta N. 2004. Detection and estimation of gas hydrates using rock physics and seismic inversion: examples from the northern deepwater gulf of mexico. The Leading Edge. 23(1):60-66. doi:10.1190/1.1645456.

Datta Gupta S, Gupta R. 2017. Importance of coloured inversion technique for thin hydrocarbon sand reservoir detection – A case in mid Cambay basin. J Geol Soc India. 90(4):485. doi:10.1007/s12594-017-0741-5.

EGPC. 1994. Nile Delta and North Sinai; fields, discoveries and hydrocarbon potentials (a comprehensive overview), Egyptian General Petroleum Corporation.

El Khadragy AA, Eysa EA, Hashim A, Abd El Kader A. 2017. Reservoir characteristics and 3D static modelling of the late miocene abu madi formation, onshore Nile delta, Egypt. J Afr Earth Sci. 132:99–108. doi:10.1016/j.jafrearsci.2017.04.032.

Gholami A. 2016. A fast automatic multichannel blind seismic inversion for high-resolution impedance recovery. Geophysics. 81(5):V357–V364. doi:10.1190/geo2015-0654.1.

Ghosh SK. 2000. Limitations on impedance inversion of band-limited reflection data. Geophysics. 65(3):951–957. doi:10.1190/1.1444791.

Goloshubin G, Tsimbalyuk Y, Privalova I, Rusakov P. 2014. Low-frequency amplitude analysis for oil detection within the middle jurassic sediments in the southern part of Western Siberia. Interpretation. 2(4):SP35–SP43. doi:10.1190/INT-2014-0040.1.

Hanafy S, Nimmagadda SL, Mahmoud SE, Mabrouk WM. 2017. New insights on structure and stratigraphic interpretation for assessing the hydrocarbon potentiality of the offshore Nile Delta basin, Egypt. J Petrol Explor Prod Technol. 7(2):317–339. doi:10.1007/s13202-016-0264-4.

Hansen TM, Mosegaard K, Pedersentatalovic R, Uldall A, Jacobsen NL. 2008. Attribute-guided well-log interpolation applied to low-frequency impedance estimation. Geophysics. 73(6):R83–R95. doi:10.1190/1.2996302.

Hardy HH, Beier RA, Gaston JD. 2003. Frequency estimates of seismic traces. Geophysics. 68(1):370–380. doi:10.1190/1.1543222.

Ismail A, Ewida HF, Al-Ibiary MG, Gammaldi S, Zollo A. 2020a. Identification of gas zones and chimneys using seismic attributes analysis at the scarab field, offshore, Nile Delta, Egypt. Pet Res. 5(1):59–69. doi:10.1016/j.ptlrs.2019.09.002.

Ismail A, Ewida HF, Al-Ibiary MG, Zollo A. 2020b. Application of AVO attributes for gas channels identification, West offshore Nile Delta, Egypt. Pet Res.Inpress.

Karimi P, Fomel S, Zhang R. 2017. Creating detailed subsurface models using predictive image-guided well-log interpolation. Interpretation 5(3):T279–T285. doi:10.1190/INT-2016-0051.1.

Khalid P, Ghazi S. 2013. Discrimination of fizz water and gas reservoir by AVO analysis: a modified approach. Acta Geod Geophys. 48(3):347e361. doi:10.1007/s40328-013-0023-7.

Khalid P, Qayyum F, Yasin Q. 2014. Data driven sequence stratigraphy of the cretaceous depositional system, Punjab Platform, Pakistan. Surv Geophys. 35 (4):1065e1088. doi:10.1007/s10712-014-9289-8.

Lancaster S, Whitcombe D. 2000a. Fast track "coloured" inversion. Expanded abstracts, 70th SEG Annual Meeting; Calgary. p. 1572–1575.

Lancaster S, Whitcombe D et al. 2000b. Fast-track 'colored'inversion: Presented at the 70th Annual International Meeting.

Marten R, Shann M, Mika J, Rothe S, Quist Y. 2004. Seismic challenges of developing the pre-Pliocene Akhen field offshore Nile Delta. Lead Edge. 23(4):314–320. doi:10.1190/1.1729228.

Maurya SP, Singh KH. 2015. June. LP and ML sparse spike inversion for reservoir characterization-a case study from Blackfoot area, Alberta, Canada. In 77th EAGE Conference and Exhibition 2015 (Vol. 2015, No. 1, pp. 1-5). European Association of Geoscientists & Engineers.

McArdle NJ, Ackers MA. 2012. Understanding seismic-thin bed responses using frequency decomposition and RGB blending. First Break. 30(1956):57–65. doi:10.3997/1365-2397.2012022.

Mohamed IA, El-mowafy HZ, Fathy M. 2015. Prediction of elastic properties using seismic prestack inversion and neural network analysis. Interpretation. 3(2):57–68. doi:10.1190/INT-2014-0139.1.

Nanda N. 2016. Seismic data interpretation and evaluation for hydrocarbon exploration and production. Berlin: Springer. doi:10.1007/978-3-319-26491-2. ISBN 978-3-319-26489-9.

Neep J. 2007. Time variant coloured inversion and spectral blueing. In: 69th EAGE Conference & Exhibition incorporating SPE EUROPEC 2007 (pp. cp-27). European Association of Geoscientists & Engineers.

Niazi M, Dahi M. 2004. Un – explored giant sandstone features in ultra – deep water, west Mediterranean, Egypt. In: AAPG International Conference; Oct 24–27; Cancun, Mexico.

Ozdemir H. 2008. Unbiased deterministic seismic inversion. 70 EAGE Conference and Exhibition Extended, London. abstracts. p.353.

Pendrel J. 2006a. Seismic inversion-a critical tool in reservoir characterization. Scand Oil-gas Mag. 5(6):19–22.

Pendrel J. 2006b. Seismic inversion — Still the best tool for reservoir characterization. CSEG Recorder. 31(1):5–12.

Pettingill HS, Weimer P. 2002. Worldwide deepwater exploration and production: past, present, and future. Lead Edge. 21(4):371–376. doi:10.1190/1.1471600.

Rastogi. 2013. Recent developments in spectral decomposition of seismic data (techniques and applications). Lead Edge. 33:164–170.

Reilly JM. 2016. Marine broadband technology: history and remaining challenges from an end-user perspective. Lead Edge. 35(4):316–321. doi:10.1190/tle35040316.1.

Rizzini A, Vezzani F, Cococcetta V, Milad G. 1978. Stratigraphy and sedimentation of a Neogene-Quaternary section in the Nile delta area. Mar Geol. 27(3–4):348–373. doi:10.1016/0025-3227(78)90038-5.

Saleh S. 2013. The role of geophysical and seismological data in evaluating the subsurface structures and tectonic trends of Nile Delta, Egypt. Arab J Geosci. 6 (9):3201–3216. doi:10.1007/s12517-012-0603-9.

Schlumberger. 1984. Chapter 1 geology of Egypt. In: Well Evaluation Conference; Egypt: Schlumberger Limited.

Ten Kroode F, Bergler S, Corsten C, de Maag JW, Strijbos F, Tijhof H. 2013. Broadband seismic data — the importance of low frequencies. Geophysics. 78(2):WA3–WA14. doi:10.1190/geo2012-0294.1.

Vandré C, Cramer B, Gerling P, Winsemann J. 2007. Natural gas formation in the western nile delta (eastern mediterranean): thermogenic versus microbial. Organic Geochemistry. 38(4):523–539. doi:10.1016/j.orggeochem.2006.12.006.

Veeken PCH, Da Silva M. 2004. Seismic inversion methods and some of their constraints: first break. 22:47–70 [accessed 2017 Oct 28]

Velzeboer CJ. 1981. The theoretical seismic reflection response of sedimentary sequences. Geophysics. 46 (6):843–853. doi:10.1190/1.1441222.

Wescott WA, Boucher PJ. 2000. Imaging submarine channels in the western Nile Delta and interpreting their paleohydraulic characteristics from 3-D seismic. Lead Edge. 19(6):580–591. doi:10.1190/1.1438662.

Worthington PF. 1985. The evolution of shaly-sand concepts in reservoir evaluation. Log Anal 26(1):23–40.

Younis A, El-Qady G, Abd Alla M, Abdel Zaher M, Khalil A, Al Ibiary M, Saraev A. 2015. AMT and CSAMT methods for hydrocarbon exploration at Nile Delta, Egypt. Arab J Geosci. 8(4):1965–1975. doi:10.1007/s12517-014-1354-6.